Solar Phys (2012) 277:185–201
DOI 10.1007/s11207-011-9881-8

Coronal Mass Ejections from Magnetic Systems Encompassing Filament Channels Without Filaments

Alexei A. Pevtsov · Olga Panasenco · Sara F. Martin

Received: 13 January 2011 / Accepted: 17 October 2011 / Published online: 15 November 2011

Abstract Well-developed filament channels may be present in the solar atmosphere even when there is no trace of filament material inside them. Such magnetic systems with filament channels without filaments can result in coronal mass ejections that might appear to have no corresponding solar surface source regions. In this case study, we analyze CMEs on 9 August 2001 and 3 March 2011 and trace their origins to magnetic systems with filament channels containing no obvious filament material on the days around the eruptions.

Keywords Coronal mass ejections, low coronal signatures · Coronal mass ejections, initiation and propagation · Magnetic fields, corona · Prominences, formation and evolution · Filaments, filament mass

1. Introduction

Coronal mass ejections (CMEs) are typically associated with flares or filament eruptions. Some studies suggest that the majority of CMEs can be traced back to filament eruptions (Subramanian and Dere, 2001). There are, however, cases of CME when no flare or filament eruption has been observed. For example, Robbrecht, Patsourakos, and Vourlidas (2009) reported a STEREO observation of a CME without a clear signature of a solar source region in the photosphere, chromosphere, or low corona. A recent statistical study by Ma *et al.* (2010) finds that about one third of CMEs observed in 2009 exhibit no signature of the eruption

Solar Flare Magnetic Fields and Plasmas
Guest Editors: Y. Fan and G.H. Fisher

A.A. Pevtsov (✉)
National Solar Observatory, Sunspot, NM 88349, USA
e-mail: apevtsov@nso.edu

O. Panasenco · S.F. Martin
Helio Research, La Crescenta, CA 91214, USA

O. Panasenco
e-mail: OlgaPanasenco@aol.com

in the low corona. We suggest that some of these CMEs "from nowhere" may originate in magnetic systems encompassing filament channels without conspicuous filaments.

A filament channel is a necessary "feature" of the chromospheric-coronal filament system (for review, see Gaizauskas, 1998). Filament channels overlay magnetic polarity reversal boundaries (also called polarity inversion lines or "neutral lines"). However, a filament channel is not a line, but a volume of space around and encompassing a filament (when it is present) or its future location. Not every polarity reversal boundary has a corresponding filament channel above and around it: a vital precondition for the formation of a filament channel is a magnetic field in it having a strong horizontal component aligned with the polarity reversal boundary (Gaizauskas, Mackay, and Harvey, 2001). In Hα, filament channels can be distinguished by "voids" of coronal mass and an anti-parallel pattern of fibrils on opposite sides of a polarity reversal boundary (Foukal, 1971; Martin, 1998; Martin, Lin, and Engvold, 2008; Martin and Panasenco, 2010; Panasenco, 2010). As summarized by Martin (1998) no fibrils cross the polarity reversal line in a fully developed filament channel. Because fibrils are field-aligned this implies that the same is probably true for magnetic field lines associated with fibrils, *i.e.*, no magnetic field lines from active region or network magnetic fields cross this polarity reversal boundary at the chromospheric level (Smith, 1968; Martin, 1990). In other words, magnetic systems associated with filament channels do not have low-lying long-lived loops across the channel except in their flaring or post-flaring state (Martin, 1990). However, long-lived loops always exist high above the channel and high above filament mass in a channel (Martin, 1990).

Filament channels are readily identifiable in He II 304 Å images during the active phase of solar cycles as dark narrow "corridors", but they are not clearly visible during the minimum of solar cycles or in circumstances when there is very little magnetic flux surrounding the polarity reversal boundary. Similarly, dark filament channels can be identified in 195 Å images (*e.g.*, Vásquez, Frazin, and Kamalabadi, 2009). Apparent coronal voids often coincide with filament channels. Not every polarity reversal boundary has a filament channel, and not every filament channel has a filament (Gaizauskas, 1998). Panasenco and Pevtsov (2010) have analyzed the evolution of a stable and apparently empty filament channel during a period of low solar activity, and found that it had some of the ingredients necessary for filament formation:

i) A magnetic neutral line.
ii) An arcade field overlying the neutral line (Martin, 1990).
iii) A coronal cavity below the arcade.

Panasenco and Pevtsov (2010) did observe an episode, when relatively hot chromospheric material (as observed in He II 304 Å) was injected into the filament channel from outside (see, Figure 1 in Panasenco and Pevtsov, 2010). However, the emission from this material rapidly disappeared as the plasma cooled down. Based on the analysis of magnetic fields, Panasenco and Pevtsov (2010) concluded that the prime reason for filaments not forming in that channel was a deficiency in the mechanism that supplies mass for filaments. Several studies have indicated that the existence of filaments is closely related to the magnetic flux cancellation rate within the filament channel (*e.g.*, Martin, Livi, and Wang, 1985; Martin, 1990; Litvinenko, 1999; Litvinenko and Martin, 1999; Wood and Martens, 2003). In a more recent study, Mackay, Gaizauskas, and Yeates (2008) confirmed that the convergence of magnetic flux leading to either flux cancellation or reconnection is required for filament formation.

Partially empty or completely empty filament channels can be observed not only in the quiet Sun, but also in active regions (Zirker *et al.*, 1997; Martin, 1998). Filament channels

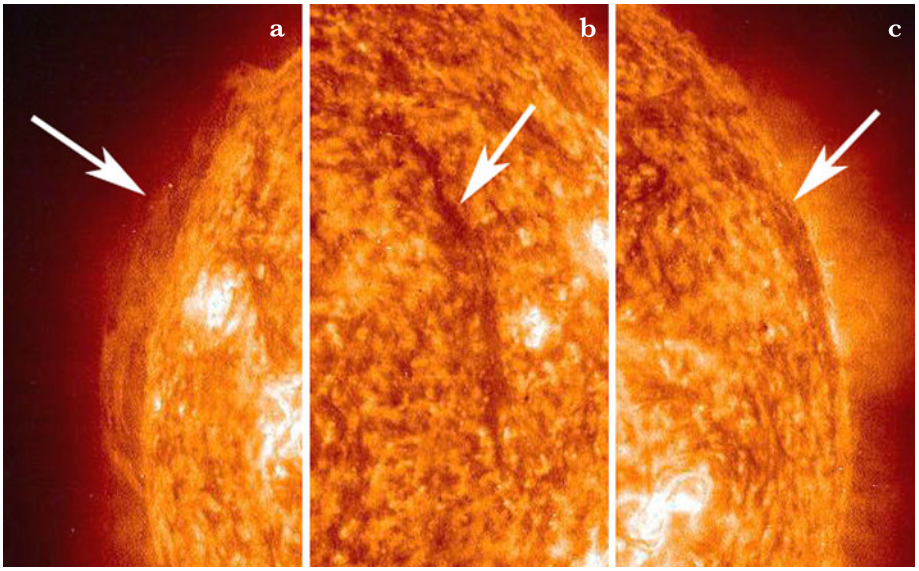

Figure 1 SOHO/EIT 304 Å images on (a) 01 August 2001 at 19:19 UT, (b) 11 August 2001 at 07:19 UT, (c) 14 August 2001 at 07:19 UT. The prominence at the east limb (a) corresponds to the filament channel observed as a dark void in 304 Å and indicated by the arrows at (b) and (c).

without filament mass in Hα in active regions are less common than among the more dispersed and lower density magnetic fields on the quiet Sun. In this paper, we present two case studies of CME originating from a magnetic system on the quiet Sun; each encompasses a filament channel largely devoid of filament mass during two to four days prior to the eruption of the filament. Informally the term "empty" has been occasionally used to refer to filament channels without the presence of a conspicuous filament material as observed in Hα and/or He II 304 Å. We cannot rule out that there could be some material present with a low-enough column density that is undetectable by observations. For example, Heinzel *et al.* (2008) have found a column density in Hα filaments in a range of $1-5 \times 10^{-5}$ g cm^{-2}. The results of their investigation suggest that if the column density is below 1×10^{-5} g cm^{-2}, no filament will be seen in Hα observations.

2. Magnetic Systems Encompassing Empty Filament Channels

2.1. Case 1: Eruption from Empty Filament Channel on 9 August 2001

Our first case of a magnetic system with an empty filament channel was observed throughout its entire disk passage during 1 – 14 August 2001. Hα observations show no indication of continuous filament material in the observed channel during the entire period of observations. He II 304 Å data also show no filament except on 1 and 2 August when a relatively hot material visible in 304 Å was periodically injected into the filament channel from one of its ends. Images taken during these two days show a prominence forming along the filament channel (see Figure 1a). However, this prominence/filament does not persist. Its material cools down rapidly and vanishes. This filament plasma behavior is similar to one described in Panasenco and Pevtsov (2010) and can be evidence of a filament channel with periodic

flow of mass along the filament channel without a clear Hα or 304 Å filament in it. As the region rotates onto the disk, the filament channel becomes visible as a dark void in EUV lines (Figure 1b, c). There are also small fragments of filament mass visible in Hα that can be identified in a few places along the filament channel. Similar mass fragments were described in Pevtsov and Neidig (2005). They might correspond to filament pillars (barbs) extending down to the chromosphere. In Hα images, higher density exists in the barbs and lower parts of filaments whereas in He II 304 Å images, the upper parts of the filament are brighter or not seen in Hα (Lin, 2004).

Figure 2a, b shows an Hα image of the solar disk and a corresponding MDI magnetogram on 6 August 2001. The white box marks the approximate location of the filament channel without a filament, and the corresponding area of the magnetic polarity reversal boundary in the photosphere. The channel has an approximate length of 50 solar degrees. It runs nearly along the solar meridian and extends from the northern to the southern hemisphere across the equator. The extrapolation of the photospheric magnetic field using a Potential Field Source Surface (PFSS) model shows the coronal arcade above the filament channel (Figure 2c). Here and in the following discussion we use the PFSS model to represent a possible magnetic connectivity in the corona. Proper modeling of the magnetic environment in the filament channel would require a more sophisticated model, and is outside the scope of this paper. From analyzing the data we conclude that this channel developed during four previous solar rotations. We estimate that at least five decaying regions from both hemispheres contributed to its formation. An example of such long-lived development of a filament channel has been described by Gaizauskas, Mackay, and Harvey (2001).

Figure 3 shows the evolution of the area marked on Figure 2a during its disk passage (to save space, data for 7 August are not shown). The first three images in Figure 3a – c (5, 6 and 8 August) show the filament channel before its eruption. The small fragments of the filament plasma are still visible in Hα on 5 and 6 August but completely disappear two days before the eruption on 9 August 2001. One can speculate that such a complete disappearance might be due to a slow rise of the magnetic system of the filament channel and the surrounding coronal loop system before its eruption accompanied by an expansion of the filament volume and a corresponding decrease in the filament density; alternatively the disappearance might be due to the quenching of the mechanism supplying filament material to the channel. As described in Pevtsov and Neidig (2005), the fragments of dark material tracing the filament channel as observed in Hα represent the filament barbs and their disappearance may be due to gradual detachment from the chromosphere during slow rise phase of the filament system before its eruption. Figure 3d shows the filament channel on 9 August, approximately seven hours after the beginning of the eruption. Figure 3e – g show partial reformation of some filament fragments after the eruption.

The filament channel just before the associated CME eruption is shown in Figure 4 (top). The void of the filament cavity observed against the disk in 195 Å is indicated by white arrows. Flare-like ribbons at the ends of the loops are rendered more visible by wavelet image processing (Figure 4, bottom). The direction of the skew of the flare loops is left-handed, which when combined with known one-to-one chiral relationships (Martin, 1998) implies dextral chirality for this filament channel. In Figure 5 the post-eruption trans-equatorial arcade is observed in the EIT 284 Å image.

A partial halo coronal mass ejection was observed in the LASCO C2 coronagraph on 9 August 2001 by 10:54 UT above NW limb (Figure 6). At first glance, coronal activity on the disk did not show any dramatic evolution suggesting the occurrence of a CME. Upon close examination, however, the changes in the corona around the long trans-equatorial filament channel provide evidence for this channel to be the key site around which the CME occurs.

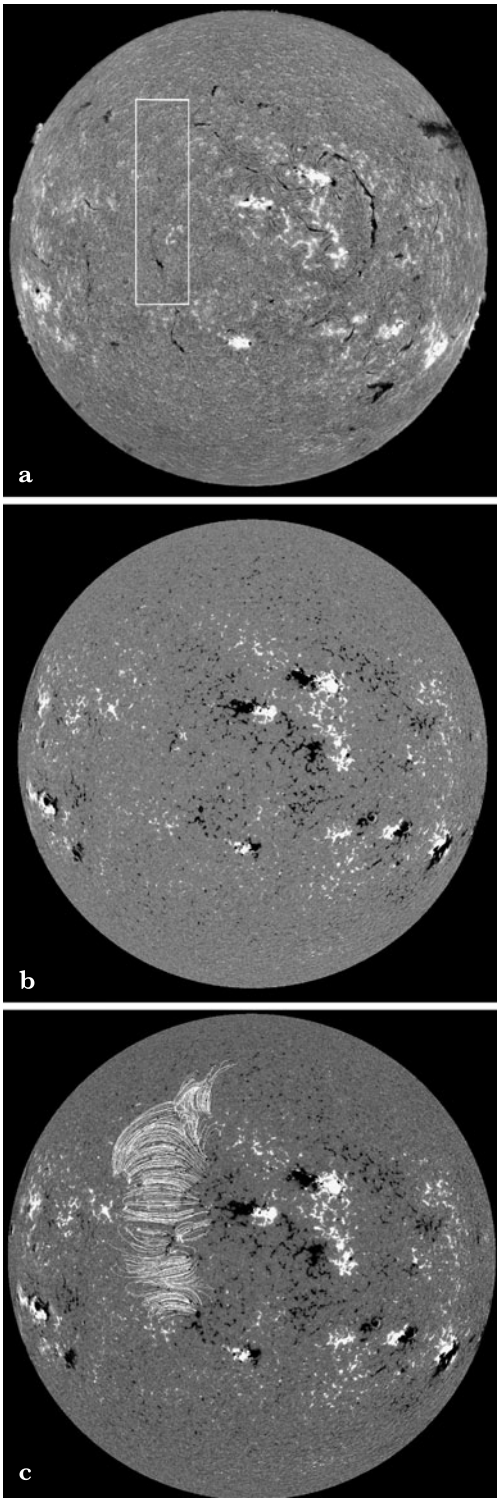

Figure 2 (a) The filament channel of the prominence in Figure 1, here marked by a white box. It was recorded in Hα at BBSO, 06 August 2001 at 16:54 UT; (b) MDI magnetogram and (c) PFSS extrapolation of the magnetic arcade above the filament channel on 06 August 2001 at 16:03 UT. While the PFSS model is an approximation of the coronal field lines, it confirms the continued existence of the channel where it appears to be empty; an overlying coronal arcade which is one of the necessary conditions for the existence of a filament channel (Martin, 1990).

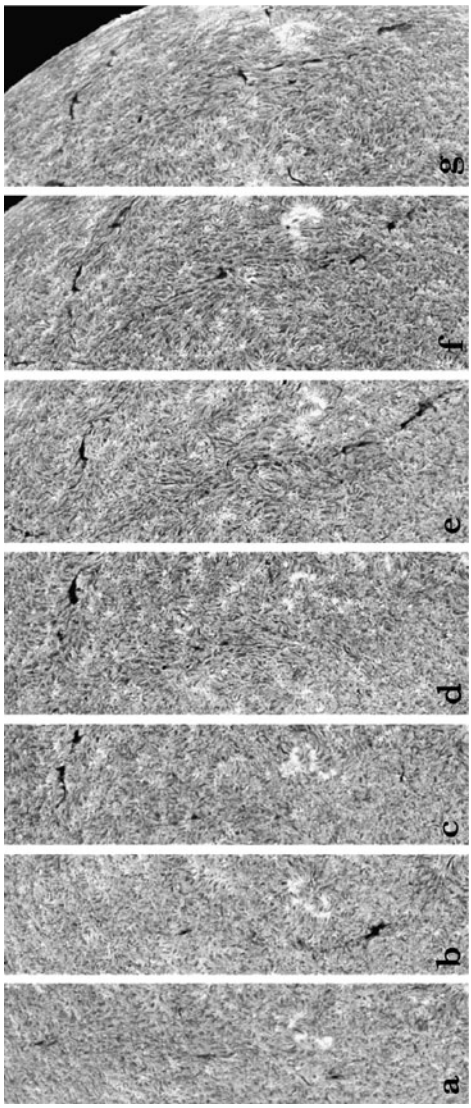

Figure 3 Chromospheric pattern of fibrils along the filament channel before and after the CME eruption on 9 August whose source region straddled this channel while it appeared to be empty. Small fragments of the filament plasma inside the channel are seen in Hα early and late in the time period 5 – 12 August 2001 (BBSO). The size of images (a) – (c) corresponds to the white box shown in Figure 2a. Images (d) – (g) were made wider since the filament channel appears more inclined with time against the rotating solar sphere.

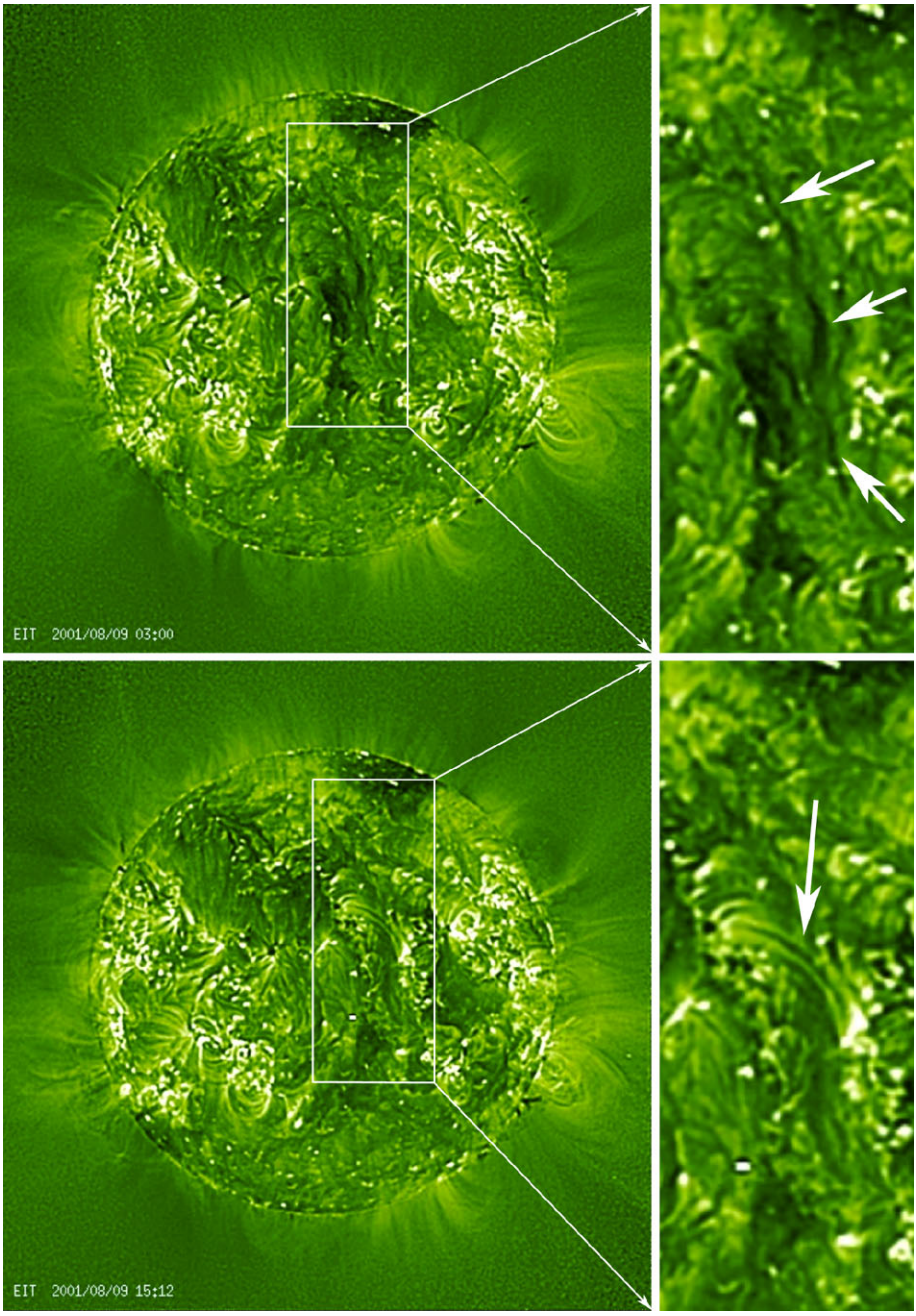

Figure 4 SOHO/EIT 195 Å wavelet-enhanced images before (top row) and after the eruption (bottom row) around 10:54 UT on 9 August. Upper row: at the left is shown the filament channel before the eruption inside a white box; at the right, white arrows point to the 195 Å dark linear feature identifying the filament channel (09 August 2001 at 03:00 UT). Bottom row: filament channel soon after the eruption; A white arrow points to flare-loop like features above the filament channel. The left-skew of these loops is evidence that the filament channel beneath has dextral chirality according to the established one-to-one solar chiral relationships. (09 August 2001 at 15:12 UT.)

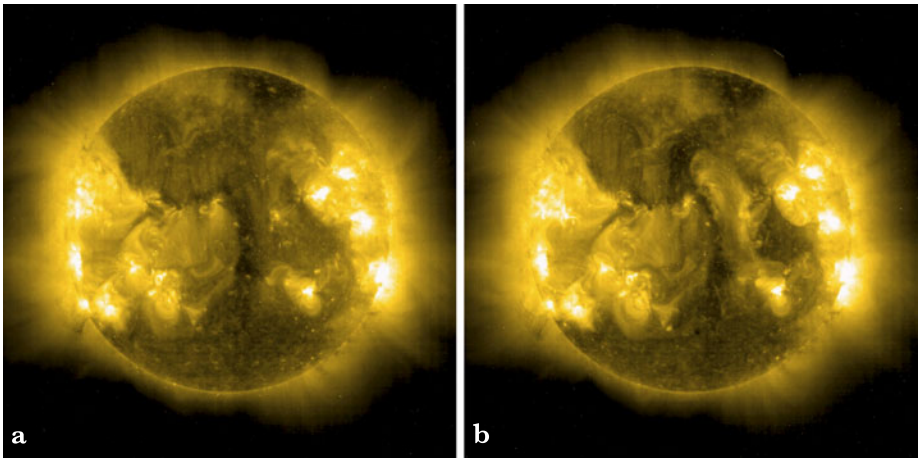

Figure 5 SOHO/EIT 284 Å images taken prior to a CME (a: 9 August 2001, 7:06 UT) and early in the eruption (b: 9 August 2001, 12:06 UT). New, post-eruption, trans-equatorial, bright, unresolved structure is clearly visible near west of an isolated coronal hole that is elongated and has a north–south orientation and crosses the equator near central meridian.

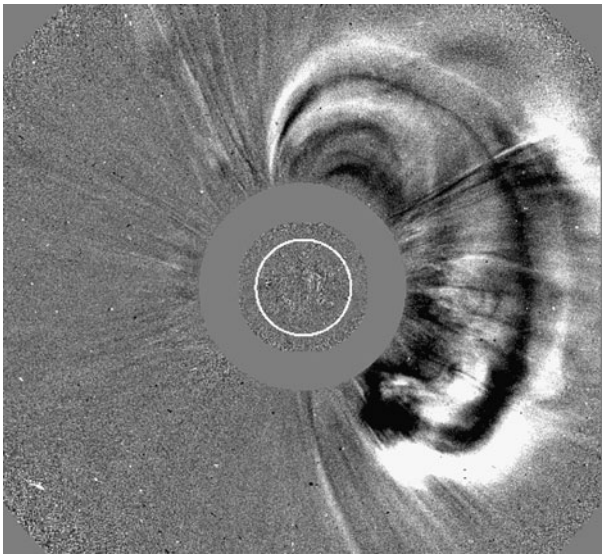

Figure 6 Although originating from near disk center, this partial halo CME is seen entirely at the west limb. This is evidence that the CME was strongly non-radial away from the elongated coronal hole nearly along the central meridian in Figure 5. (SOHO/LASCO C2 09 August 2001 at 12:30 UT.)

The timing of events in this first case, observed on the solar disk in EIT 195 Å data, provides observational evidence for a CME originating from above and around the trans-equatorial filament channel situated near the disk center on 9 August. No filament material was observed in this channel in Hα or He II 304 Å spectral lines. Therefore, we refer to it as an "empty" filament channel at the time of the associated CME and during the preceding day. A wide post-eruption trans-equatorial set of "loops" crossing the filament channel was observed in EIT 284 Å (Figure 5b) and soft X-ray (*Yohkoh*) images, which indicates the presence of high temperature coronal plasma formed at the sides of the filament channel during the CME formation. Hα images show no brightenings along the filament channel that

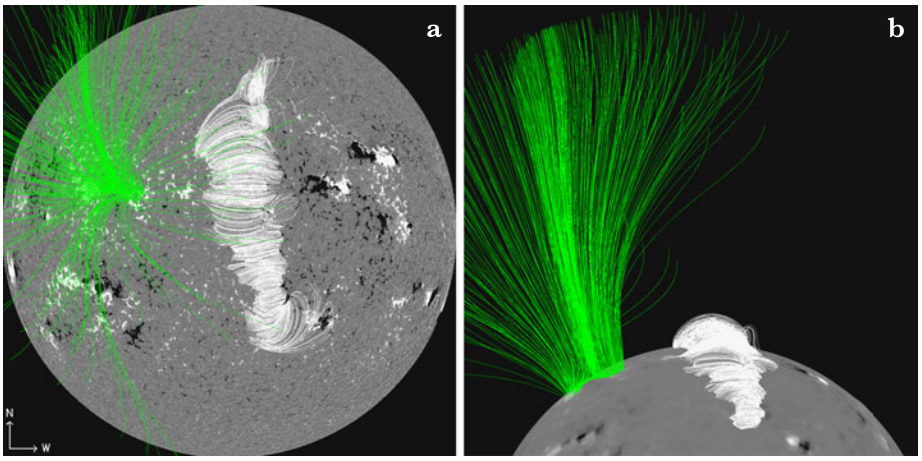

Figure 7 Magnetic field lines from the PFSS model on 08 August 2001 18:04 UT (a) "on disk" and (b) "off limb" projections. White lines correspond to closed field lines of the arcade overlying the filament channel; the green lines are open field lines originating in an isolated coronal hole east of the filament channel. Under these circumstances, any CME originating from the coronal arcade is expected to be non-radial to the west away from the magnetic field of the coronal hole as indicated in Figure 6.

could indicate a reconnection process if a "flux rope" structure was formed at the beginning of the eruption. On the other hand, we do see two compact brightenings near the northern and southern ends of the filament channel in the early stages of the eruption (no figure is shown). These brightenings suggest that a horizontal structure with at least one continuous field line connecting the two ends of the filament channel has already been present at the very early stages of the eruption. Additionally, EIT 304 Å and 195 Å images show weak brightenings on opposite sides of the filament channel near its middle part, as well as thin bright loops reminiscent of post-flare loops. This evolution observed during the early stages of the eruption around this filament channel shows several aspects typical for the classical two-ribbon flare scenario, albeit with much weaker intensity.

The potential field extrapolation (Figures 2c and 7) reveals the presence of a magnetic arcade above the filament channel. The magnetic polarity of the footpoints on the eastern side of the arcade is positive, the same as that of the coronal hole situated to the east of the filament channel. In the LASCO C2 coronagraph, the CME front can be clearly identified in images taken at 10:54 UT. Using difference images, we manually traced the CME's front in five consecutive images. The change in height of the CME front (F_{CME}) with time (t) was fitted by second degree polynomial to arrive at an initial speed of 257 km s^{-1} and an acceleration of ≈ 0.024 km s^{-2} relative to its first appearance at 10:54 UT: $F_{CME} = (257 \pm 20) \cdot t + (0.012 \pm 0.002) \cdot t^2$. By the time the CME left the LASCO C2 field of view, the CME front was moving with a speed of about 450 – 480 km s^{-1} in the image plane.

Although the CME had originated around the filament channel near the disk center, the CME was observed propagating mostly from the west limb of the Sun. We suggest, based on use of the PFSS modeling (Figure 7), that the CME had non-radial motion that is consistent with deflection toward the west by the open magnetic field of an isolated coronal hole. Deflection of CMEs by coronal hole boundaries has been reported by several researchers (*e.g.*, Gopalswamy *et al.*, 2003, 2009; Cremades and Bothmer, 2004; Panasenco *et al.*, 2011). Figure 7 shows that the approximate configuration of the coronal hole, situated farther away

from the filament channel, would allow deflection of the CME to take place high in the corona.

Between 12 August (about 10:40 UT) and 13 August ($\approx$ 11:00 UT), *in situ* measurements from ACE and WIND spacecraft registered a passage of an interplanetary CME (ICME). Taking the first indication of the ICME disturbance in ACE data as the ICME front yields an average ICME velocity of about 580 km s^{-1}, which seems to be in general agreement with estimates based on LASCO observations. The ICME had a complicated structure with multiple reversals in the direction of all three components of its magnetic field. Due to this complexity, we did not attempt fitting any axi-symmetric model of magnetic cloud to ACE data.

Geomagnetic measurements of the A_p-index show an onset of a major geomagnetic storm at approximately 22:40 UT on 12 August (A_p-index = 56 at storm's maximum at 4:30:43 UT on 13 August). Using the calculated time difference ($\approx$ 3.5 days) between the estimated CME eruption and the beginning of geomagnetic storm yields an average speed of the CME of about 500 km s^{-1}, which, again, is in agreement with CME speed measured from LASCO C2 images. This general agreement between CME speeds measured near the Sun, at the location of ACE, and at 1 AU supports our conjecture for a causal relation between this CME and the ensuing geomagnetic storm.

Observations from the LASCO C3 coronagraph show two CMEs on 9 August 2001 (one from the west limb studied here, and the other leaving the east limb at approximately 22:18 UT). The measured speed of the CME associated with the empty filament channel suggests that the interplanetary CME observed by ACE and WIND is caused by the CME from the west limb. However, the size of the ICME at the locations of ACE and WIND is significantly larger than one that can be inferred from a relatively short-duration geomagnetic storm. Also, the timing between, the ICME onset at the location of ACE and WIND and the onset of the geomagnetic storm, suggests that this ICME had largely missed the Earth. Thus, the geomagnetic storm observed on 13 August can be associated with one of the "threads" of the ICME observed at ACE and WIND. The complex magnetic topology of the ICME could be explained as the result of interactions between CME flux rope structure originating from the magnetic field over the filament channel and the magnetic field of the coronal hole.

2.2. Case 2: Eruption from a Filament Channel on 3 March 2011

A CME without a clearly identifiable source region on the disk was observed on 3 March 2011 by the two STEREO and the SOHO spacecraft. The separation angle between STEREO A and B was about 182° allowing observation of the CME from its two opposite sides while the front view was deduced from SOHO/LASCO data (see Figure 8). Similar to case 1, there initially was no clearly identifiable source region for this CME. By applying a geometric triangulation method to STEREO A and B data, we have estimated the heliographic coordinates of the source region as $\approx$S35° $\pm$ 10°, W15° $\pm$ 10°. Figure 9 shows the derived area against SDO/AIA 193 Å, SDO/HMI magnetogram and Hα BBSO images. Additional inspection of this data around the triangulated heliographic coordinates places the source of the CME on a filament channel without a definite filament in the southern hemisphere. Figure 10 shows three consecutive images during the early and late stages of eruption. White arrows in Figure 10 indicate the two-ribbon flare-like emission developing in the corona on both sides of filament channel at the time of the overlying eruption. The filament channel is clearly identifiable in Hα images (Figure 11). On Figure 11 (upper panel), the filament channel can be seen as a slightly darker curved "path" that begins south-west

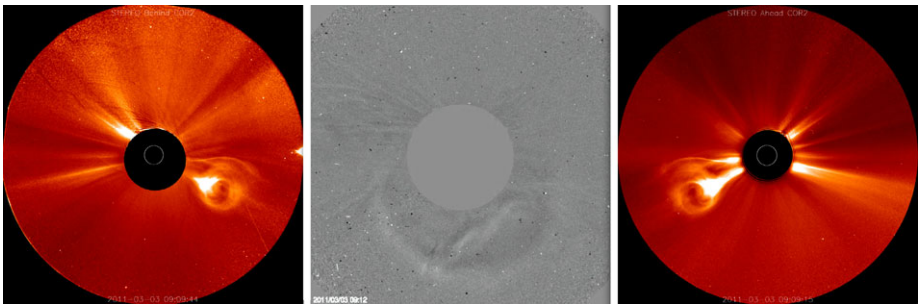

Figure 8 Left and right panels: the CME observed by the COR2 instrument onboard STEREO-B and STEREO-A, respectively, on 03 March 2011 at 09:09 UT. The simultaneous observations of a CME on both STEREO A and B in these orientations can only be due to an event with its origin near the middle of the solar disk. Middle panel: Half-halo CME observed by SOHO/LASCO C2 03 March 2011 at 09:12 UT.

(below and to the right) of bright active region plage, and "arches" below the active region to the east. On Figure 11 (lower panel), the location of the filament channel is marked by dark fragments of filament material. The background of the channel appears to be slightly darker on average than the surrounding areas (Figure 11, top) due to the relative absence of plagettes or bright areas in the channel. In images of higher spatial resolution than these, one would typically be able to see some of the fibrils in the channel. Especially near the filament segments and along the boundary between the opposite polarities, fibrils align with the polarity reversal boundary or have a component aligned with the polarity reversal boundary.

As the characteristics of observed changes are gradual and minor in the chromosphere and corona, we suggest there is gradual loss of equilibrium prior to the onset of this CME. As one possibility, the new flux emergence in the vicinity of the filament channel may lead to the destabilization of filaments contained within them (*e.g.*, Bruzek, 1952). The *Bruzek relationship* of specific erupting quiescent filaments to the birth of new active regions has been verified in subsequent studies (Feynman and Martin, 1995; Wang and Sheeley, 1999; Feynman and Ruzmaikin, 2004; Jing *et al.*, 2004; Balasubramaniam *et al.*, 2011). The eruption on 3 March 2011 happened at the time when a new strong active region began to emerge northwest from the filament channel. Figure 12 shows PFSS magnetic field line extrapolations in the vicinity of the filament channel before and after the new active region's emergence.

Our application of the model allows us to deduce whether the new flux could or does interact with the coronal fields that straddle the filament channel. It is clear from Figure 12, as new magnetic flux emerges, some of its field lines connect to preexisting flux of another active region. In turn, this leads to establishing new magnetic connections between the mature active region and one of polarities of magnetic arcade overlying filament channel. Thus, new large flux emergence could result in a change to the overall magnetic configuration around the filament channel and a weakening or decrease of the overlying coronal arcade field by transferring connectivity to the newly emerged adjacent magnetic flux. Similar changes in magnetic connectivity have been recently observed by Balasubramaniam *et al.* (2011) prior to a filament eruption. We should emphasize, however, that we use field lines extrapolated from the PFSS model only as a graphical representation of possible change in the topology. To properly model this development, a more sophisticated model would be needed that takes into account possible non-potentiality of the magnetic field around filament channel. It is worth noticing, however, a recent paper by Liu, Zhang, and Su (2011)

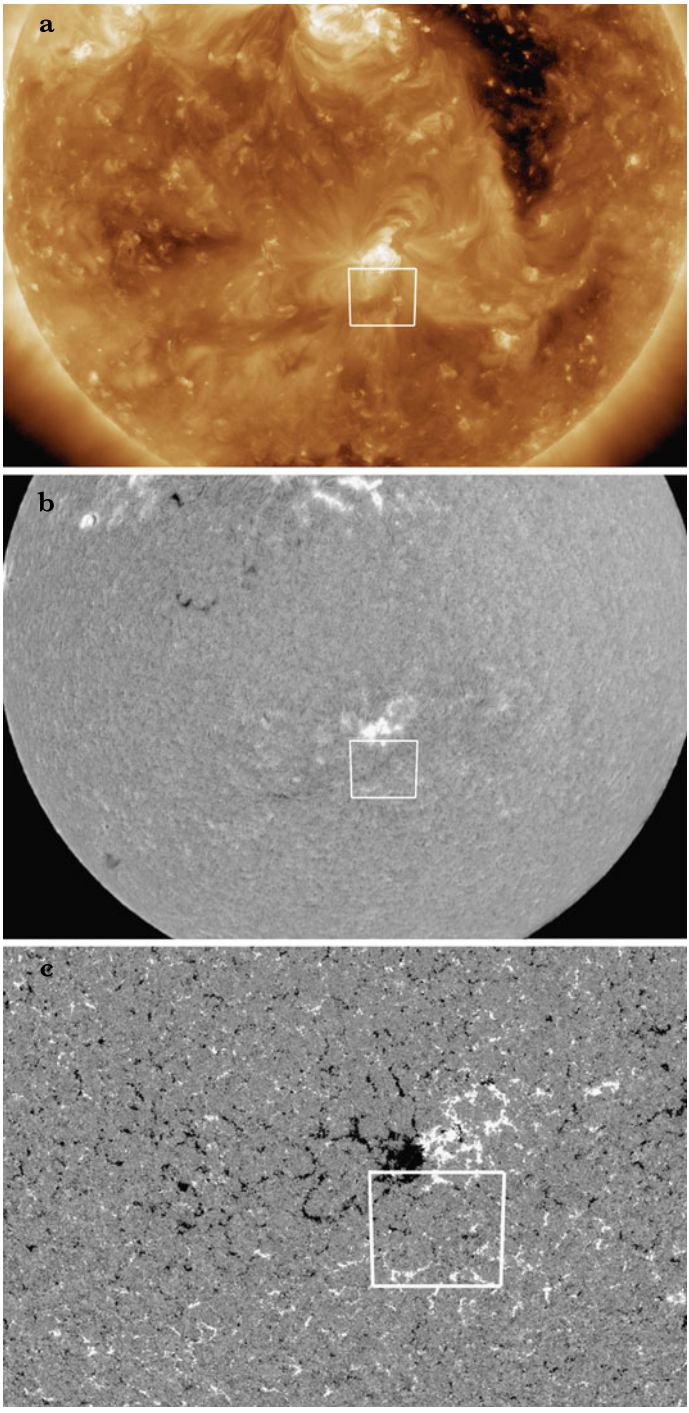

Figure 9 The source region of the CME in Figure 8 is identified with the filament channel and polarity boundary within the white boxes. From top to bottom (all on 2 March 2011): (a) SDO/AIA 193 Å at 18:00 UT, (b) BBSO Hα at 17:56 UT, and (c) SDO/HMI at 17:53 UT.

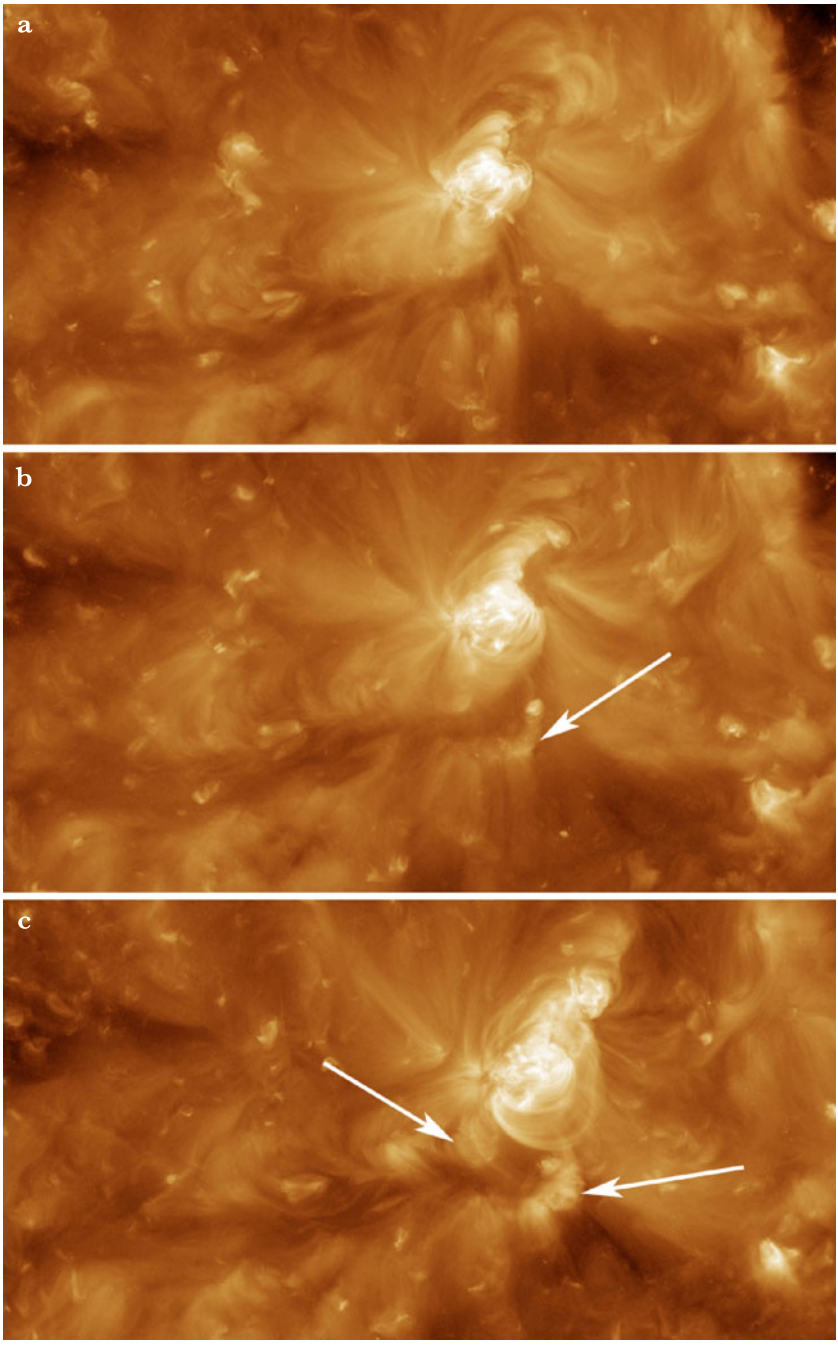

Figure 10 Brightenings reminiscent of a weak two-ribbon flare were observed after the slow CME eruption by SDO/AIA 193 Å: (a) 14:00 UT, 2 March 2011, (b) 21:15 UT, 2 March 2011, and (c) 09:15 UT, 3 March 2011. Unlike post-flare loops, these coronal structures on each side of the channel (shown by the white arrows) do not appear to straddle the empty filament channel although they develop together with a small transient coronal hole southward from channel.

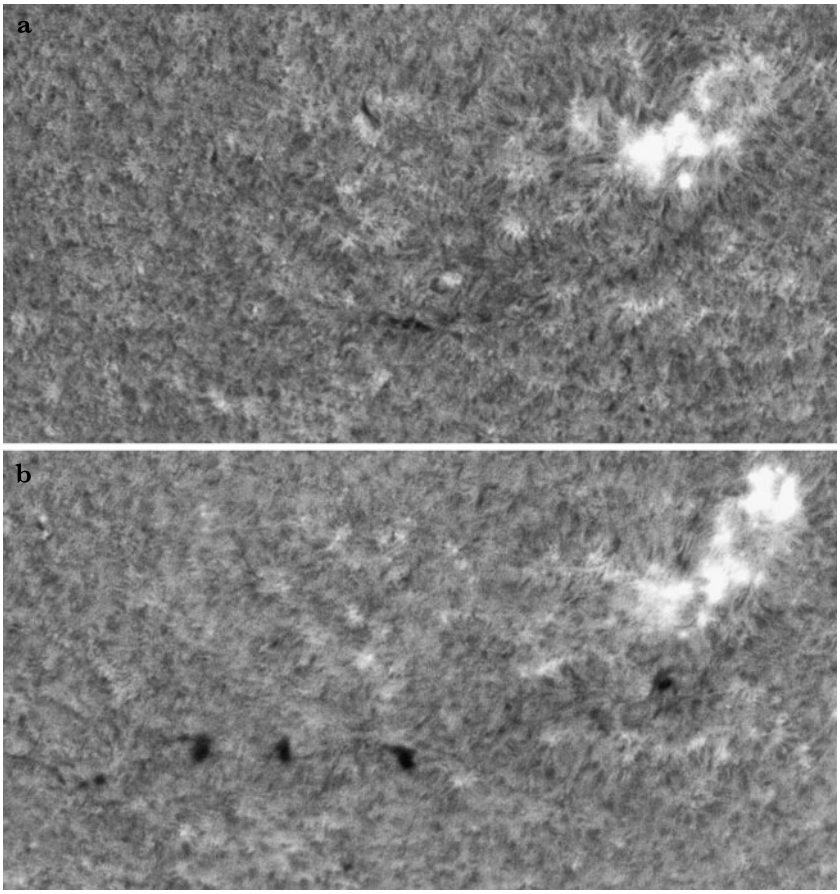

Figure 11 Chromospheric pattern of plagettes and fibrils along the filament channel (a) before and (b) after the flare-like brightenings and CME that both straddle this filament channel. Small fragments of the filament plasma are seen here inside this relatively empty channel observed in Hα (BBSO). Panel (a) shows data from 2 March 2011 at 17:56 UT, and (b) is for 3 March 2011 at 17:56 UT.

who compared the configuration of coronal magnetic fields from PFSS and non-linear force-free (NLFFF) models. They found that NLFFF and PFSS extrapolations agree reasonably well at the heights > 2000 km above the photosphere. Wang and Sheeley (1999) used the PFSS model to investigate the effects of a newly emerging flux on coronal arcades overlying filaments. They concluded that emergence of a new magnetic flux in the vicinity of filaments will weaken the coronal arcade above filaments and may lead to their eruption. The situation shown on Figure 12 appears to be in agreement with conclusions of Wang and Sheeley (1999).

Unlike the eruption of 9 August 2001 (our case 1), this CME did not produce an ICME at the ACE spacecraft location. No geomagnetic storm associated with this CME was observed either. Given the observed trajectory, we suggest that the CME passed the Earth orbit below the ecliptic plane.

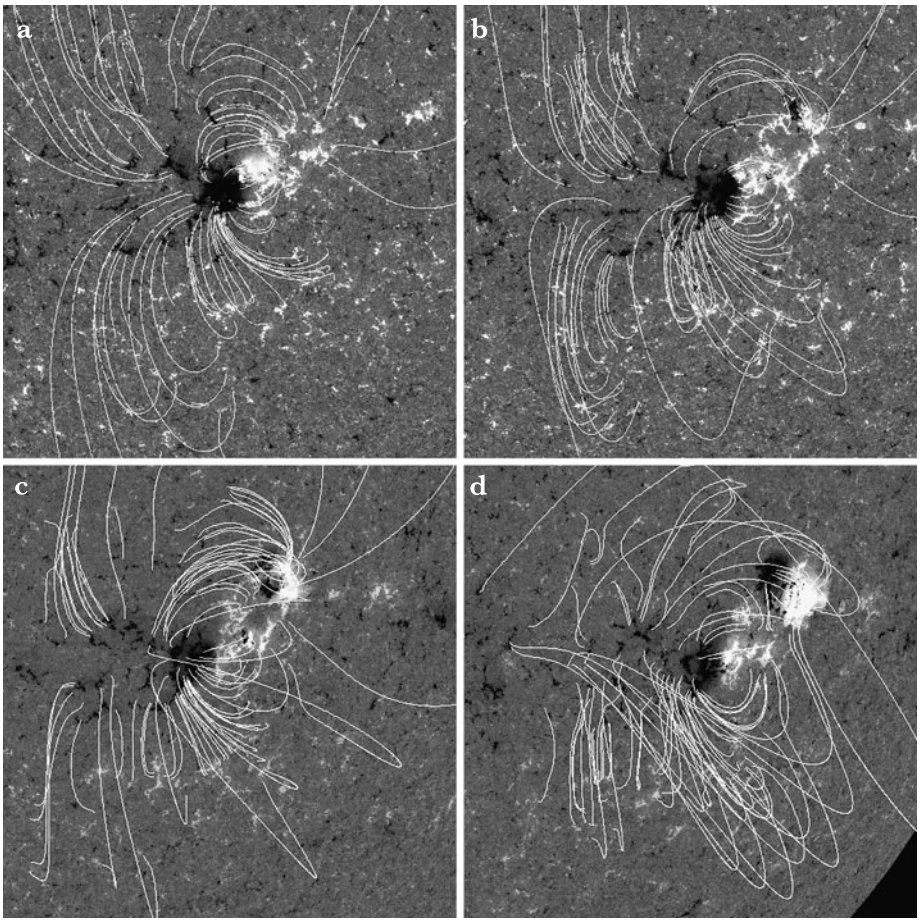

Figure 12 SDO/HMI magnetograms and corresponding magnetic field lines from the PFSS model before (panel (a), 2 March 2011) and during the emergence of the new active region (panels (b) 3 March 2011, (c) 4 March 2011, and (d) 5 March 2011. Time in all panels corresponds to 06:10 UT). While the PFSS model is not expected to exactly represent conditions of solar magnetic fields, it provides evidence that at least the depicted amount of change most likely occurred in association with the emerging active region and that these changes would be consistent with altering the magnetic configuration sufficiently to result in the flare in Figure 10 and the associated CME in Figure 8.

3. Discussion

Two examples described in this article indicate that CMEs can erupt from relatively empty filament channels, and that such CMEs can produce both geoeffective and non-geoeffective CMEs. In the absence of a clearly identifiable source region on the disk, successful detection of the origin of such "stealth" CMEs requires a wide and complex examination of the filament channels as candidate sources, together with the monitoring of new flux emergence in the vicinity of filament channels.

CMEs from magnetic systems encompassing filament channels without conspicuous filaments, similar to the ones described in this article, may explain CMEs that appear as having no obvious source regions on the solar disk. Close examination of EIT 304 Å images taken

around the time of the event reported in Robbrecht, Patsourakos, and Vourlidas (2009) shows a compact brightening similar to footpoint brightenings characteristic of the phase of maximum acceleration of erupting filaments (Wang, Muglach, and Kliem, 2009). Also, after the CME, we see the formation of two elongated fragments of the chromospheric filament material inside the channel. These fragments are indicative of the location of the chromospheric filament channel, which apparently did not contain dense material prior to the CME. In our opinion, these post-eruption features suggest that the CME described in Robbrecht, Patsourakos, and Vourlidas (2009) could also have originated from a magnetic system with a filament channel without a conspicuous filament. For additional examples of CMEs without obvious solar surface source regions, we refer the reader to the events described in Bhatnagar (1996), McAllister *et al.* (1996), and Shakhovskaya, Abramenko, and Yurchyshyn (2002). Another more recent example is the CME eruption on 23 May 2010 at about 16:00 UT observed by *Solar Dynamics Observatory* (SDO). Preliminary analysis of data suggests that this CME may have also originated from a filament channel without an obvious filament.

Acknowledgements The authors thank M. Velli for reading and discussions on the manuscript. A.P.'s work had benefited from partial support provided by NASA's NNH09AL04I inter-agency transfer. O.P. and S.M. were supported by NSF grants 0837915 and 0852249. National Solar Observatory (NSO) is operated by the Association of Universities for Research in Astronomy, AURA Inc. under cooperative agreement with the National Science Foundation.

References

Balasubramaniam, K.S., Pevtsov, A.A., Cliver, E.W., Martin, S.F., Panasenco, O.: 2011, *Astrophys. J.* in press.
Bhatnagar, A.: 1996, *Astrophys. Space Sci.* **243**, 105.
Bruzek, A.: 1952, *Z. Astrophys.* **31**, 99.
Cremades, H., Bothmer, V.: 2004, *Astron. Astrophys.* **422**, 307.
Feynman, J., Martin, S.: 1995, *J. Geophys. Res.* **100**(43), 3355.
Feynman, J., Ruzmaikin, A.: 2004, *Solar Phys.* **219**, 301.
Foukal, P.: 1971, *Solar Phys.* **19**, 59.
Jing, J., Yurchyshyn, V.B., Yang, G., Xu, Y., Wang, H.: 2004, *Astrophys. J.* **614**, 1054.
Heinzel, P., Schmieder, B., Fárník, F., Schwartz, P., Labrosse, N., Kotrč, P., Anzer, U., Molodij, G., Berlicki, A., DeLuca, E.E., Golub, L., Watanabe, T., Berger, T.: 2008, *Astrophys. J.* **686**, 1383.
Gaizauskas, V.: 1998, In: Webb, D., Rust, D., Schmieder, B. (eds.) *IAU Colloq. 167: New Perspectives on Solar Prominences*, *ASP Conf. Series* **150**, Astron. Soc. Pac., San Francisco, 257.
Gaizauskas, V., Mackay, D.H., Harvey, K.L.: 2001, *Astrophys. J.* **558**, 888.
Gopalswamy, N., Shimojo, M., Lu, W., Yashiro, S., Shibasaki, K., Howard, R.A.: 2003, *Astrophys. J.* **586**, 562.
Gopalswamy, N., Mäkelä, P., Xie, H., Akiyama, S., Yashiro, S.: 2009, *J. Geophys. Res.-Atmos.* **114**, A22.
Lin, Y.: 2004, Ph.D. Thesis, Institute of Theoretical Astrophysics, University of Oslo.
Litvinenko, Y.E.: 1999, *Astrophys. J.* **515**, 435.
Litvinenko, Y.E., Martin, S.F.: 1999, *Solar Phys.* **190**, 45.
Liu, S., Zhang, H.Q., Su, J.T.: 2011, *Solar Phys.* **270**, 89.
Ma, S., Attrill, G.D.R., Golub, L., Lin, J.: 2010, *Astrophys. J.* **722**, 289.
Mackay, D.H., Gaizauskas, V., Yeates, A.R.: 2008, *Solar Phys.* **248**, 51.
Martin, S.F.: 1990, In: Rudzjak, V., Tandberg-Hanssen, E. (eds.) *IAU Colloq. 117: Dynamics of Quiescent Prominences*, Springer, Berlin, 1.
Martin, S.F.: 1998, *Solar Phys.* **182**, 107.
Martin, S.F., Panasenco, O.: 2010, *Mem. Soc. Astron. Ital.* **81**, 662.
Martin, S.F., Livi, S.H.B., Wang, J.: 1985, *Aust. J. Phys.* **38**, 929.
Martin, S.F., Lin, Y., Engvold, O.: 2008, *Solar Phys.* **250**, 31.
McAllister, A.H., Dryer, M., McIntosh, P., Singer, H., Weiss, L.: 1996, *J. Geophys. Res.* **101**, 13497.
Panasenco, O.: 2010, *Mem. Soc. Astron. Ital.* **81**, 673.
Panasenco, O., Pevtsov, A.: 2010, In: Cranmer, S.R., Hoeksema, J.T., Kohl, J.L. (eds.) *SOHO-23: Understanding a Peculiar Solar Minimum*, *ASP Conf. Series* **428**, Astron. Soc. Pac., San Francisco, 123.

Panasenco, O., Martin, S., Joshi, A.D., Srivastava, N.: 2011, *J. Atmos. Solar-Terr. Phys.* **73**, 1077.
Pevtsov, A.A., Neidig, D.: 2005, In: Sankarasubramaniam, K.S., Penn, M.J., Pevtsov, A.A. (eds.) *Large Scale Structures and their Role in Solar Activity*, *ASP Conf. Series* **346**, Astron. Soc. Pac., San Francisco, 219.
Robbrecht, E., Patsourakos, S., Vourlidas, A.: 2009, *Astrophys. J.* **701**, 283.
Shakhovskaya, A.N., Abramenko, V.I., Yurchyshyn, V.B.: 2002, *Solar Phys.* **207**, 369.
Smith, S.F.: 1968, In: Kiepenheuer, K.O. (ed.) *Structure and Development of Solar Active Regions*, *IAU Symp.* **35**, Reidel, Dordrecht, 267.
Subramanian, P., Dere, K.P.: 2001, *Astrophys. J.* **561**, 372.
Vásquez, A.M., Frazin, R.A., Kamalabadi, F.: 2009, *Solar Phys.* **256**, 73.
Wang, Y.-M., Sheeley, N.R.: 1999, *Astrophys. J.* **510**, L157.
Wang, Y.-M., Muglach, K., Kliem, B.: 2009, *Astrophys. J.* **699**, 133.
Wood, P., Martens, P.: 2003, *Solar Phys.* **218**, 123.
Zirker, J.B., Martin, S.F., Harvey, K., Gaizauskas, V.: 1997, *Solar Phys.* **175**, 27.